



Article

Antitumor Activities of a Humanized Cancer-Specific Anti-HER2 Monoclonal Antibody, humH₂Mab-250 in Human Breast Cancer Xenografts

Mika K. Kaneko ¹ , Hiroyuki Suzuki ^{1,*} , Tomokazu Ohishi ^{2,3} , Takuro Nakamura ¹, Miyuki Yanaka ¹, Tomohiro Tanaka ¹ and Yukinari Kato ^{1,*}

¹ Department of Antibody Drug Development, Tohoku University Graduate School of Medicine, 2-1 Seiryomachi, Aoba-ku, Sendai 980-8575, Miyagi, Japan; mika.kaneko.d4@tohoku.ac.jp (M.K.K.); takuro.nakamura.a2@tohoku.ac.jp (T.N.); miyuki.yanaka.c5@tohoku.ac.jp (M.Y.); tomohiro.tanaka.b5@tohoku.ac.jp (T.T.)

² Institute of Microbial Chemistry (BIKAKEN), Numazu, Microbial Chemistry Research Foundation, 18-24 Miyamoto, Numazu 410-0301, Shizuoka, Japan; ohishit@bikaken.or.jp

³ Institute of Microbial Chemistry (BIKAKEN), Laboratory of Oncology, Microbial Chemistry Research Foundation, 3-14-23 Kamiosaki, Shinagawa-ku 141-0021, Tokyo, Japan

* Correspondence: hiroyuki.suzuki.b4@tohoku.ac.jp (H.S.); yukinari.kato.e6@tohoku.ac.jp (Y.K.); Tel.: +81-22-717-8207 (H.S. & Y.K.)

Abstract: Monoclonal antibody (mAb) and cell-based immunotherapies represent cutting-edge strategies for cancer treatment. However, safety concerns persist due to the potential targeting of normal cells that express reactive antigens. Therefore, it is crucial to develop cancer-specific mAbs (CasMabs) that can bind to cancer-specific antigens and exhibit antitumor activity in vivo, thereby reducing the risk of adverse effects. We previously screened mAbs targeting human epidermal growth factor receptor 2 (HER2) and successfully developed a cancer-specific anti-HER2 mAb, H₂Mab-250/H₂CasMab-2 (mouse IgG₁, kappa). In this study, we assessed both the in vitro and in vivo antitumor efficacy of the humanized H₂Mab-250 (humH₂Mab-250). Although humH₂Mab-250 showed lower reactivity to HER2-overexpressed Chinese hamster ovary-K1 (CHO/HER2) and breast cancer cell lines (BT-474 and SK-BR-3) than trastuzumab in flow cytometry, both humH₂Mab-250 and trastuzumab showed similar antibody-dependent cellular cytotoxicity (ADCC) against CHO/HER2 and the breast cancer cell lines in the presence of effector splenocytes. In addition, humH₂Mab-250 exhibited significant complement-dependent cellular cytotoxicity (CDC) in CHO/HER2 and the breast cancer cell lines compared to trastuzumab. Furthermore, humH₂Mab-250 possesses compatible in vivo antitumor effects against CHO/HER2 and breast cancer xenografts with trastuzumab. These findings highlight the distinct roles of ADCC and CDC in the antitumor effects of humH₂Mab-250 and trastuzumab and suggest a potential direction for the clinical development of humH₂Mab-250 for HER2-positive tumors.

Keywords: cancer-specific monoclonal antibody; HER2; ADCC; CDC; xenograft; breast cancer



Academic Editor: Valentina De Falco

Received: 29 December 2024

Revised: 22 January 2025

Accepted: 24 January 2025

Published: 26 January 2025

Citation: Kaneko, M.K.; Suzuki, H.; Ohishi, T.; Nakamura, T.; Yanaka, M.; Tanaka, T.; Kato, Y. Antitumor Activities of a Humanized Cancer-Specific Anti-HER2 Monoclonal Antibody, humH₂Mab-250 in Human Breast Cancer Xenografts. *Int. J. Mol. Sci.* **2025**, *26*, 1079. <https://doi.org/10.3390/ijms26031079>

Copyright: © 2025 by the authors.

Licensee MDPI, Basel, Switzerland.

This article is an open access article distributed under the terms and conditions of the Creative Commons Attribution (CC BY) license (<https://creativecommons.org/licenses/by/4.0/>).

1. Introduction

Monoclonal antibody (mAb)-based therapeutics are essential for treating various diseases. The U.S. Food and Drug Administration (FDA) approved the first therapeutic mAb, Orthoclone OKT3 (mouse anti-CD3 mAb), for kidney transplantation rejection in 1986 [1]. However, the first-generation mouse mAbs tested in clinical trials had limited effectiveness

due to their immunogenicity and poor effector functions [2]. Patients developed human anti-mouse antibody responses, which caused the rapid clearance of the therapeutic mAbs from the body and restricted the number of possible treatment doses [2]. The creation of engineered chimeric, humanized, and fully human mAbs has uncovered several valuable applications for antibody-based therapies [3,4].

In mAb therapy for solid tumors, the FDA approved trastuzumab for human epidermal growth factor receptor 2 (HER2)-positive breast cancer in 1998 [5]. HER2-positive breast cancer is defined by circumferential membrane staining that is complete, intense, and in >10% of tumor cells in immunohistochemistry (IHC 3+) and/or in situ hybridization (ISH)-positive [6]. Trastuzumab is a humanized mAb by inserting the complementarity determining regions (CDRs) of mouse anti-HER2 mAb (clone 4D5) into the framework of a consensus human IgG₁ [7]. Trastuzumab exhibited antitumor efficacy against HER2-positive breast cancer xenograft in monotherapy or combination therapy with chemotherapy [8–10]. The clinical efficacy of trastuzumab is mediated by the immunologic engagement [11]. Trastuzumab exerts antibody-dependent cellular cytotoxicity (ADCC) upon the binding to Fcγ receptors on natural killer cells or macrophages [11]. The combination therapy of trastuzumab with chemotherapy improves the progression-free survival and overall survival in HER2-positive breast cancer patients with metastasis [12]. Currently, HER2 overexpression and activating mutations have been observed in gastric and gastroesophageal cancers [13,14], endometrial cancers [15,16], non-small-cell lung cancers [17,18], and ovarian cancers [19].

Trastuzumab-deruxtecan (T-DXd), a trastuzumab-based antibody–drug conjugate (ADC), has been developed and received the FDA approval [20]. T-DXd has demonstrated superior efficacy not only in HER2-positive breast cancers [21,22] but also in HER2-low (IHC 1+ or IHC 2+/ISH-non-positive) advanced breast cancers [23] and HER2-mutant non-small-cell lung cancers [24]. Given that approximately half of all breast cancers are classified as HER2-low, a substantial number of patients are expected to benefit from T-DXd therapy [25]. Although T-DXd is generally well-tolerated and rarely causes severe toxicity, studies have consistently linked it to the development of cardiac toxicity. While this issue is not clinically significant in most cases, baseline cardiac evaluation, regular monitoring, and early detection of cardiac adverse events are still crucial for T-DXd. Since HER2 plays a critical role in normal heart development and homeostasis [26,27], on-target, off-tumor toxicity in the heart would cause adverse effects. Therefore, management of the specificity of mAb to tumors will be required for further optimization.

Although 97 ADCs have been evaluated in clinical trials since 2000, 81 trials were terminated due to the lack of efficacy (32 agents) and safety issues (32 agents) [28]. On-target, off-tumor toxicity is thought to be a cause of adverse effects when the target antigen is expressed in normal cells. Therefore, selecting mAbs that specifically recognize cancer-related epitopes is critical to reducing unwanted side effects.

Activation of the complement-dependent cytotoxicity (CDC) pathway has been suggested as a mechanism to enhance the therapeutic effectiveness of antitumor mAbs [29]. It is one of the reported mechanisms for B-cell targeting anti-CD20 mAbs, such as ofatumumab and rituximab [30–33]. Trastuzumab mediates antitumor effects through various mechanisms but is unable to induce CDC in HER2-positive cells in the presence of human serum [34,35]. The activation of the classical complement pathway is regulated by various factors, including the size and density of the antigen, which influence the geometry of the antigen-antibody complex needed for effective C1q binding [29]. For optimal CDC activity, the Fc domains of antibodies within antigen-antibody clusters must be organized in a hexameric structure, which creates a geometry that enhances C1q binding and complement activation [29]. Approaches to improve CDC, such as antibody hexamerization [36,37] and

Fc mutations [38], have shown promise in boosting antitumor activity in preclinical studies. For example, hexamerization was used to develop an anti-CD37 biparatopic antibody with enhanced in vitro CDC activity [39].

We previously generated cancer-specific anti-HER2 mAbs, H₂Mab-214/H₂CasMab-1 [40] and H₂Mab-250/H₂CasMab-2 [41], selected from 278 anti-HER2 clones, using HER2 expressed by glioblastoma LN229 cells as the target antigen. Interestingly, both H₂Mab-214 and H₂Mab-250 showed no reactivity toward spontaneously immortalized normal epithelial cells, such as HaCaT and MCF 10A [40,41]. Moreover, H₂Mab-250 exhibited no binding to normal epithelial cells derived from various tissues, including the mammary gland, kidney proximal tubule, gingiva, colon, thymus, cornea, and lung bronchus [41]. In contrast, most anti-HER2 mAbs, including trastuzumab, reacted with both cancer and normal epithelial cells [41]. Furthermore, H₂Mab-250 exhibited no reactivity with the normal heart in IHC [41]. Epitope mapping identified Trp614 in HER2 extracellular domain 4 (ECD4) as a critical determinant for H₂Mab-250 recognition [41]. H₂Mab-214 was also found to target a similar epitope as H₂Mab-250, with structural analysis suggesting that H₂Mab-214 binds to a misfolded region of the β -sheet in HER2-ECD4 [32]. This suggests that localized misfolding within the cysteine-rich portion of ECD4 contributes to the cancer specificity of H₂Mab-214. Additionally, we engineered mouse IgG_{2a} and mouse-human chimeric versions of H₂Mab-250. Both antibodies demonstrated antitumor activity against breast cancer xenografts in vivo, performing comparably to trastuzumab despite lower binding affinity and effector function activation in vitro [42,43].

This study evaluates the ADCC, CDC, and antitumor efficacy of the humanized version of H₂Mab-250 (humH₂Mab-250).

2. Results

2.1. Humanized Anti-HER2 mAb (humH₂Mab-250)

We previously established an anti-HER2 mAb (H₂Mab-250; mouse IgG₁, kappa) by immunization with the HER2 ectodomain produced by glioblastoma LN229 cells [41]. H₂Mab-250 was shown to be useful for flow cytometry [41]. In this study, we engineered a humanized H₂Mab-250 (humH₂Mab-250) by fusing the V_H and V_L CDRs of H₂Mab-250 with the C_H and C_L chains of human IgG₁, respectively (Figure 1A). We also engineered trastuzumab and humCvMab-62 (a control human IgG₁) from CvMab-62 (mouse IgG₁, an anti-SARS-CoV-2 spike protein S2 subunit mAb) [44]. Recombinant mAbs were produced by fucosyltransferase 8-knockout ExpiCHO-S cells to produce the defucosylated form of mAbs. The defucosylation of mAbs has been reported to potentiate the binding to the Fc γ RIIIa receptor, which results in increased ADCC activity by natural killer (NK) cells or macrophages [45,46]. In reduced conditions, we confirmed the purity of mAbs by SDS-PAGE (Figure 1B).

As shown in Figure 2, humH₂Mab-250 and trastuzumab reacted with CHO/HER2 (HER2-overexpressed CHO-K1) cells in a dose-dependent manner (Figure 2A) but not with parental CHO-K1 cells (Figure 2B). Furthermore, humH₂Mab-250 and trastuzumab reacted with HER2-positive breast cancer BT-474 (Figure 2C) and SK-BR-3 (Figure 2D). The reactivity of humH₂Mab-250 to HER2-positive cells was similar compared to that of parental mAb, H₂Mab-250 [41]. We also confirmed no reactivity of humH₂Mab-250 to HaCaT (human keratinocyte), 293FT (embryonic kidney), and MCF 10A (mammary gland epithelial cells) (Supplementary Figure S1) as we previously showed that using H₂Mab-250 [41]. The humCvMab-62 did not react with CHO-K1, CHO/HER2, BT-474, and SK-BR-3 at 10 μ g/mL (Supplementary Figure S2). We used humCvMab-62 as a control human IgG₁.

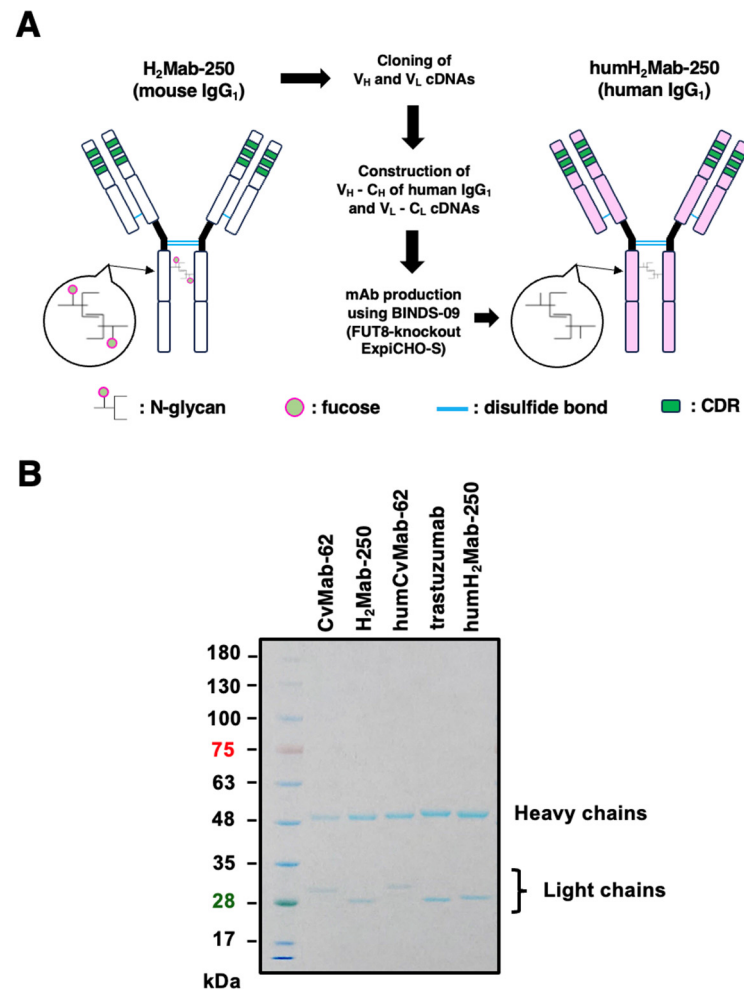


Figure 1. Generation of a humanized IgG₁ mAb, humH₂Mab-250. **(A)** The CDRs of H₂Mab-250 V_H and V_L were cloned into human IgG₁ and human kappa chains, respectively. The humH₂Mab-250 was produced by BINDS-09 (fucosyltransferase 8-knockout ExpiCHO-S) cells, as described in materials and methods. **(B)** Confirmation of the purified mAbs. MAbs (2 µg) were treated with sodium dodecyl sulfate sample buffer containing 2-mercaptoethanol. Proteins were separated on 5–20% polyacrylamide gel and stained by Bio-Safe CBB G-250.

2.2. ADCC and CDC by humH₂Mab-250 Against HER2-Positive Cells

We next examined whether humH₂Mab-250 exerted ADCC activity against CHO/HER2 cells. Since human IgG₁ can bind to all activating mouse Fcγ receptors and induce ADCC in the presence of mouse NK cells and macrophages [47], we evaluated ADCC of humH₂Mab-250 and trastuzumab in the presence of mouse splenocytes as effector cells. As shown in Figure 3A, humH₂Mab-250 and trastuzumab induced ADCC in the presence of effector splenocytes against CHO/HER2 (19.9 and 23.0% cytotoxicity, respectively) more effectively than the control human IgG₁ (5.9% cytotoxicity; $p < 0.05$). Furthermore, both humH₂Mab-250 and trastuzumab induced ADCC against BT-474 (8.8 and 9.9% cytotoxicity, respectively) more effectively than the control human IgG₁ (1.7% cytotoxicity; $p < 0.05$, Figure 3B). Both humH₂Mab-250 and trastuzumab also induced ADCC against SK-BR-3 (5.5 and 5.8% cytotoxicity, respectively) more effectively than the control human IgG₁ (1.4% cytotoxicity; $p < 0.05$, Figure 3C). We also examined the ADCC activity against CHO/HER2, BT-474, and SK-BR-3 cells in the presence of human NK cells. As shown in Supplementary Figure S3, both humH₂Mab-250 and trastuzumab induced significant ADCC against CHO/HER2. Additionally, trastuzumab induced significant ADCC against BT-474, and humH₂Mab-250 induced significant ADCC against SK-BR-3. These results suggest that humH₂Mab-250

exerted compatible ADCC activities against HER2-positive cells by mouse splenocytes compared to that by human NK cells.

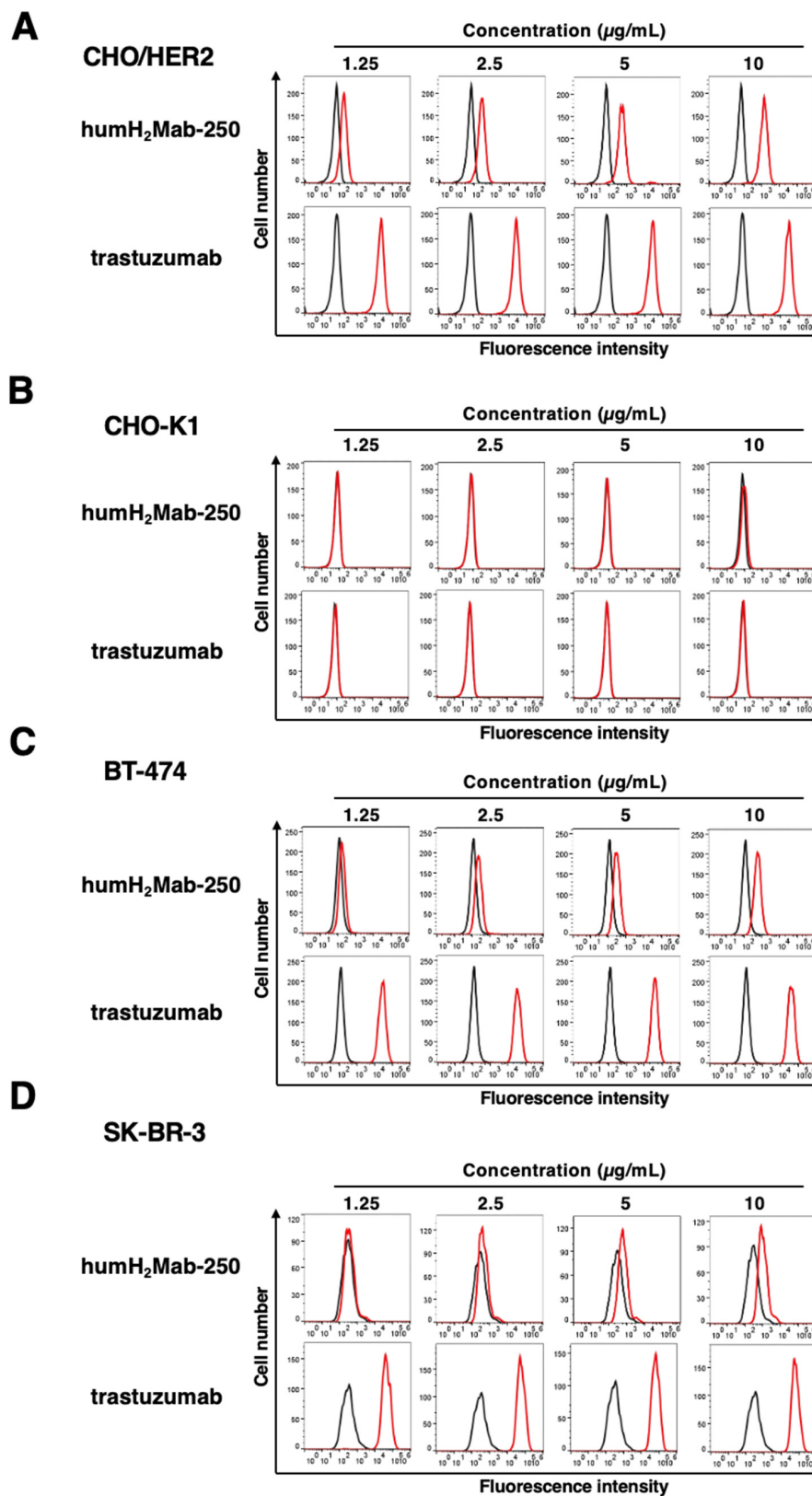


Figure 2. Flow cytometry using humH₂Mab-250 and trastuzumab. CHO/HER2 (A), CHO-K1 (B), BT-474 (C), and SK-BR-3 (D) cells were treated with humH₂Mab-250 (1.25 to 10 $\mu\text{g/mL}$, red line), trastuzumab (1.25 to 10 $\mu\text{g/mL}$, red line), or buffer control (black line), followed by anti-human IgG conjugated with FITC. The SA3800 Cell Analyzer was used to analyze fluorescence data.

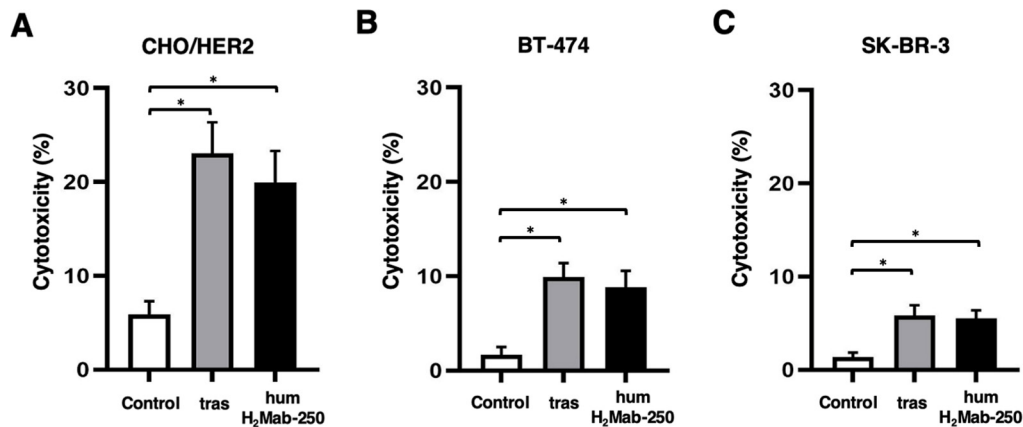


Figure 3. The ADCC is mediated by humH₂Mab-250 and trastuzumab. Calcein-labeled CHO/HER2 (A), BT-474 (B), and SK-BR-3 (C) were treated with trastuzumab (tras), humH₂Mab-250 or control human IgG₁ in the presence of effector splenocytes. The cytotoxicity was determined by the release of calcein into the medium. Values are shown as the mean \pm SEM. Asterisks indicate statistical significance (* $p < 0.05$; one-way ANOVA Tukey's multiple comparisons test).

We investigated CDC by humH₂Mab-250 and trastuzumab against CHO/HER2. As shown in Figure 4A, humH₂Mab-250 showed a significant CDC in the presence of complements against CHO/HER2 (14.4% cytotoxicity) more effectively than the control human IgG₁ (3.5% cytotoxicity; $p < 0.05$). In contrast, trastuzumab did not show a significant difference compared to the control in CHO/HER2 cells ($p = 0.09$, Figure 4A). Furthermore, both humH₂Mab-250 and trastuzumab induced CDC against BT-474 (9.7 and 7.7% cytotoxicity, respectively) more effectively than the control human IgG₁ (1.8% cytotoxicity; $p < 0.05$ [trastuzumab], $p < 0.01$ [humH₂Mab-250], Figure 4B). In contrast, both humH₂Mab-250 and trastuzumab did not induce CDC against SK-BR-3 significantly (Figure 4C).

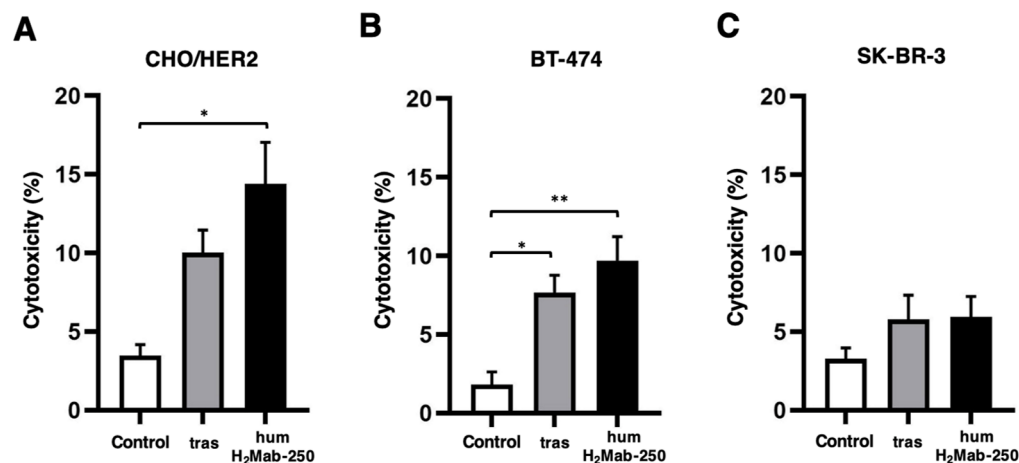


Figure 4. Evaluation of CDC by humH₂Mab-250 and trastuzumab. Calcein-labeled CHO/HER2 (A), BT-474 (B), and SK-BR-3 (C) were treated with trastuzumab (tras), humH₂Mab-250 or control human IgG₁ in the presence of complements. The cytotoxicity was determined by the release of calcein into the medium. Values are shown as the mean \pm SEM. Asterisks indicate statistical significance (* $p < 0.05$ and ** $p < 0.01$; one-way ANOVA Tukey's multiple comparisons test).

2.3. Antitumor Effects of humH₂Mab-250 Against CHO/HER2, BT-474, and SK-BR-3 Xenografts

In the preclinical studies of trastuzumab, the antitumor effect was proved using human breast cancer xenografts in athymic mice without human-derived effector cells [8–10]. To compare the antitumor effect of humH₂Mab-250 with trastuzumab, we employed a similar experimental condition. In the CHO/HER2, BT-474, and SK-BR-3 xenograft tumor-

bearing BALB/c nude mice, humH₂Mab-250, trastuzumab, or control human IgG₁ was intraperitoneally administered on days 7, 14, and 21. The humH₂Mab-250 treatment significantly reduced the volume of CHO/HER2 xenografts on days 14 ($p < 0.05$), 21 ($p < 0.05$), and 28 ($p < 0.01$) compared with that induced by the control human IgG₁ (Figure 5A). The humH₂Mab-250 treatment also exhibited a significant reduction in the volume of BT-474 xenografts on days 10 ($p < 0.05$), 14 ($p < 0.01$), 21 ($p < 0.01$), 23 ($p < 0.05$), and 27 ($p < 0.01$) compared with that induced by the control human IgG₁ (Figure 5B). The humH₂Mab-250 treatment caused a significant reduction in SK-BR-3 xenograft on days 21 ($p < 0.01$), 23 ($p < 0.01$), and 27 ($p < 0.01$) compared with that induced by the control human IgG₁ (Figure 5C). The humH₂Mab-250 exhibited a comparable antitumor effect against CHO/HER2, BT-474, and SK-BR-3 with trastuzumab (Figure 5A, Figure 5B, and Figure 5C, respectively). The humH₂Mab-250 and trastuzumab treatments resulted in a 94% and 93% decrease in CHO/HER2 xenograft weight compared with that induced by the control human IgG₁ on day 28 (Figure 5D). No antitumor effects were observed in CHO-K1 xenograft treated with humH₂Mab-250 and trastuzumab (Supplementary Figure S4).

The humH₂Mab-250 and trastuzumab treatments resulted in similar decreases (57%) in BT-474 xenograft weight compared with that induced by the control human IgG₁ on day 27 (Figure 5E). The humH₂Mab-250 and trastuzumab treatments also resulted in a 54% and 55% decrease in SK-BR-3 xenograft weight compared with that induced by the control human IgG₁ on day 27 (Figure 5F).

Figure 5G–I demonstrate the CHO/HER2, BT-474, and SK-BR-3 xenografts resected on day 27, respectively. Body weight loss was rarely observed in CHO/HER2, BT-474, and SK-BR-3 xenograft-bearing mice treated with humH₂Mab-250, trastuzumab, or control human IgG₁ (Figure 5J–L).

Supplementary Figure S5 presents the body appearance of CHO/HER2, BT-474, and SK-BR-3 xenograft-inoculated mice treated with humH₂Mab-250, trastuzumab, or control human IgG₁.

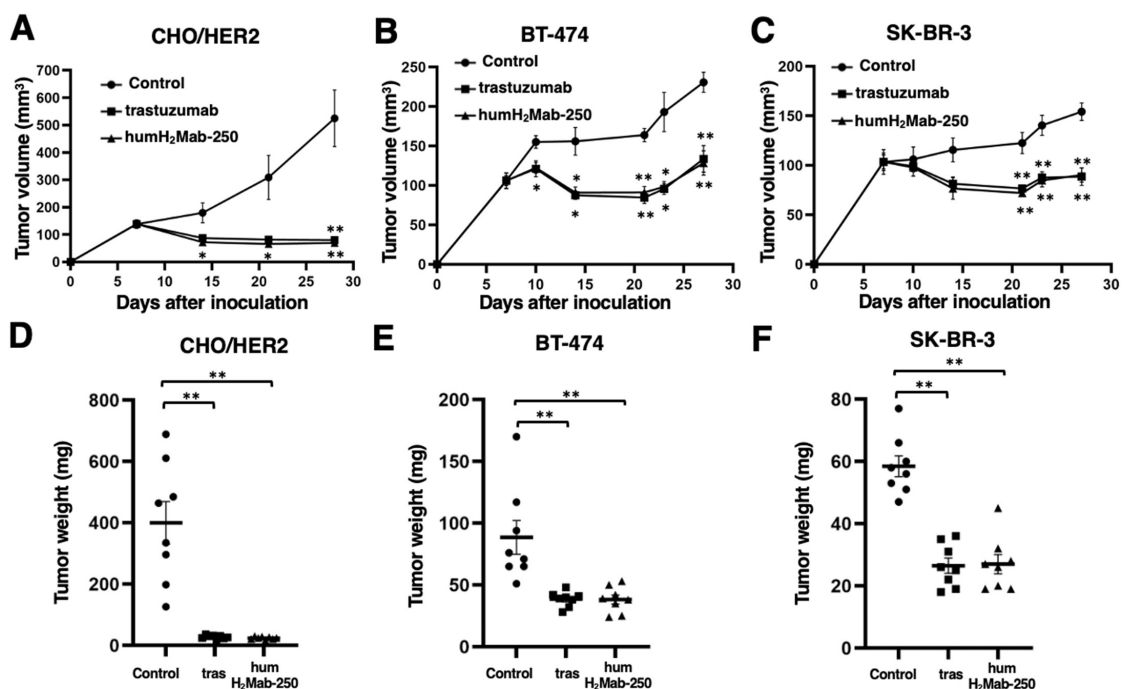


Figure 5. Cont.

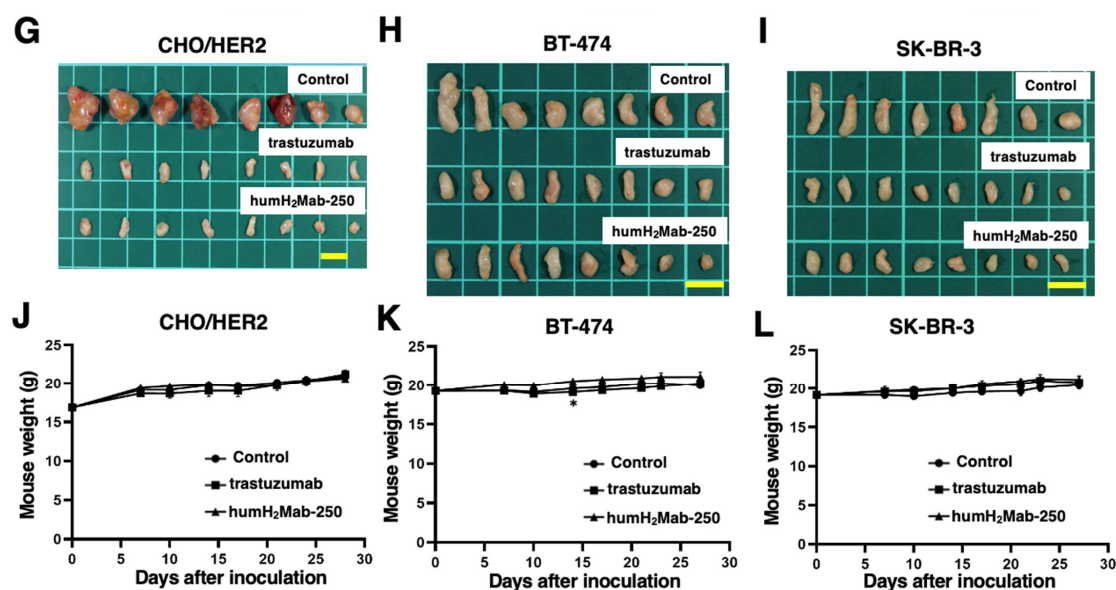


Figure 5. Antitumor activity of humH₂Mab-250 against CHO/HER2, BT-474, and SK-BR-3 xenografts. (A–C) CHO/HER2 (A), BT-474 (B), and SK-BR-3 (C) cells were subcutaneously injected into BALB/c nude mice (day 0). On day 7, 100 µg of humH₂Mab-250, trastuzumab, or control human IgG₁ was administered. Additional antibodies were administered on days 14 and 21. The tumor volume was measured on the indicated days. Values are presented as the mean ± SEM. * $p < 0.05$ and ** $p < 0.01$; Two-way ANOVA Tukey’s multiple comparisons test. (D–F) The CHO/HER2 (D), BT-474 (E), and SK-BR-3 (F) xenograft tumor weight on day 28 (CHO/HER2) or day 27 (BT-474 and SK-BR-3). Values are represented as the mean ± SEM. ** $p < 0.01$; one-way ANOVA Tukey’s multiple comparisons test). (G–I) The appearance of CHO/HER2 (G), BT-474 (H), and SK-BR-3 (I) xenograft tumors (scale bar, 1 cm). (J–L) Body weight of CHO/HER2 (J), BT-474 (K), and SK-BR-3 (L) xenograft-bearing mice treated with humH₂Mab-250, trastuzumab, or control human IgG₁. Values are presented as the mean ± SEM. * $p < 0.05$ (Two-way ANOVA with Tukey’s multiple comparisons test).

3. Discussion

In the development of mAbs for cancer treatment, identifying and validating suitable antigenic targets is crucial [4]. To achieve a favorable therapeutic index and minimize on-target toxicity, the ideal target antigens should be highly expressed in tumors with minimal or no presence in normal tissues. However, finding such optimal targets remains a significant challenge. Technologies like bispecific antibodies, defucosylated antibodies, and ADCs have improved antibody efficacy and advanced cancer therapy. However, the issue of on-target toxicity—caused by antigen recognition in normal cells—still persists.

In this study, humH₂Mab-250 exhibited antitumor efficacy in mouse xenograft models (Figure 5). The humH₂Mab-250 demonstrated enhanced CDC activity in the presence of complement (Figure 4). Therefore, the formation of the MAC (membrane attack complex) is thought to form efficiently on the cell surface. Various factors, such as antigen size and density, influence the activation of the classical complement pathway [48]. Moreover, the geometry of the antigen–mAb complex facilitates efficient binding of C1q, which initiates the classical complement activation pathway [29]. Since IgG antibodies can form ordered hexamers upon binding to their target antigen on cell surfaces [36,49], the structure of the humH₂Mab-250-HER2 complex may allow sufficient access for complement proteins to trigger CDC. Further research is needed to understand better the mechanisms by which humH₂Mab-250 induces CDC.

CasMabs targeting HER2 (clones H₂Mab-214 [40] and H₂Mab-250 [41]) were identified through screening for reactive with cancer and non-reactive with normal cells in flow cytometry. Both CasMabs demonstrated antitumor effects in mouse xenograft models

with their recombinant mouse IgG_{2a} or mouse-human chimeric IgG₁ mAbs [40,42,43]. The recognition mechanism of H₂Mab-214 was elucidated by X-ray crystallography, revealing that it binds to a locally misfolded structure in the ECD4 of HER2, which typically forms a β -sheet [40]. Since H₂Mab-250 possesses a similar binding epitope with H₂Mab-214 [50], H₂Mab-250 or humH₂Mab-250 would recognize the cancer-specific epitope of HER2. Therefore, structural analysis of the H₂Mab-250 and tumor-derived HER2 complex will be critical for further understanding the mechanism of cancer-specific recognition compared with that of H₂Mab-214.

H₂Mab-250 was also converted to a single chain variable fragment (scFv), developed to chimeric antigen receptor (CAR)-T cell therapy. A phase I clinical trial for patients with HER2-positive advanced solid tumors is underway in the US (NCT06241456). In CD19-positive relapsed/refractory B-cell leukemia patients who have previously been treated with CD19 CAR-T possessing mouse-derived scFv (mCD19 CAR-T), the reinfusion of mCD19 CAR-T cells may not be practical due to the development of antibodies against the anti-mouse scFv [51,52]. To address the immunogenicity, humanized CD19 CAR-T cell therapy was developed and showed a clinical benefit for the patients who had received mCD19 CAR-T therapy [53]. The scFv from humH₂Mab-250 could be another option for CAR-T therapy targeting cancer-specific HER2.

Both trastuzumab and H₂Mab-250 recognize the ECD4 of HER2. Trastuzumab recognizes a wider epitope of HER2 (residues 579–625) [50]. In contrast, H₂Mab-250 recognizes a narrow and membrane-proximal epitope of HER2 (residues 613–617) [41]. Significantly, the reactivity wholly disappeared in a HER2 (W614A) mutant [41]. Furthermore, H₂Mab-250 showed a lower binding affinity ($\sim 10^{-9}$ M) than trastuzumab ($\sim 10^{-10}$ M) to HER2 ectodomain [43]. Several studies have shown that lower affinity CARs against CD19, glypican-3, and disialoganglioside (GD2) avoid excessive stimulation and exhaustion in the presence of low antigen burden, which leads to durable antitumor responses [54–56]. Furthermore, a novel anti-CD19 mAb, h1218 that possesses a membrane-proximal epitope and exhibits faster on/off rates compared to clinically approved FMC63, was developed [57]. The h1218-CAR-T showed increased killing of B-cell malignancies compared to FMC63-CAR-T. Mechanistically, the h1218-CAR-T has reduced activation-induced cell death compared to FMC63-CAR-T owing to faster on/off rates [57]. These results support that the low affinity and membrane-proximal epitope possessing H₂Mab-250 CAR-T exhibited effectiveness in a preclinical study [58]. Furthermore, the formation of the MAC at the membrane-proximal region is considered essential to attack the plasma membrane of tumor cells. Among mAbs targeting CD20, ofatumumab has been shown to possess potent CDC activity compared to rituximab [30,59], which might be due to the membrane-proximal epitope and kinetics of binding to CD20 for C1q binding [31,59]. Further studies are essential to reveal the relationship between the epitope and CDC in HER2-targeting mAbs.

4. Materials and Methods

4.1. Cell Lines

BT-474, SK-BR-3, MCF 10A, and CHO-K1 cell lines were sourced from the American Type Culture Collection (Manassas, VA, USA). 293FT and HaCaT cells were obtained from Thermo Fisher Scientific Inc. (Thermo, Waltham, MA, USA) and Cell Lines Service GmbH (Eppelheim, Germany), respectively. These cells were maintained as described previously [41].

4.2. Recombinant mAb Production

To generate a humanized anti-human HER2 mAb (humH₂Mab-250), the CDRs of H₂Mab-250 V_H and V_L were cloned into human IgG₁ and human kappa chain expression vectors [60], respectively. We transfected the antibody expression vectors of humH₂Mab-250 into BINDS-09 (fucosyltransferase 8-knockout ExpiCHO-S) cells using the ExpiCHO-S Expression System (Thermo). We purified humH₂Mab-250 using Ab-Capcher (ProteNova Co., Ltd., Kagawa, Japan). Trastuzumab was produced as described previously [43]. As a control human IgG₁ mAb, humCvMab-62 was produced from CvMab-62 [44] using the abovementioned method. To confirm the purity of mAbs, they were treated with sodium dodecyl sulfate sample buffer containing 2-mercaptoethanol, separated on 5–20% polyacrylamide gel (FUJIFILM Wako Pure Chemical Corporation, Osaka, Japan), and stained by Bio-Safe CBB G-250 (Bio-Rad Laboratories, Inc., Berkeley, CA, USA).

4.3. Animal Experiments

To assess the antitumor effects of humH₂Mab-250, animal experiments were conducted according to the guidelines of the Declaration of Helsinki and approved by the Institutional Committee for Experiments at the Institute of Microbial Chemistry (approval no. 2024-059).

4.4. Flow Cytometry

CHO-K1, CHO/HER2, BT-474, and SK-BR-3 cells were harvested using 0.25% trypsin and 1 mM ethylenediaminetetraacetic acid (EDTA; Nacalai Tesque, Inc., Kyoto, Japan). The cells (1×10^5 cells per sample) were incubated with blocking buffer (control) (0.1% BSA in PBS), trastuzumab, or humH₂Mab-250 for 30 min at 4 °C. Following this, the cells were treated with fluorescein isothiocyanate (FITC)-conjugated anti-human IgG (1:2000; Sigma-Aldrich Corp., St. Louis, MO, USA) for 30 min at 4 °C. Fluorescence data were collected using the SA3800 Cell Analyzer (Sony Corp., Tokyo, Japan) and analyzed with FlowJo software (version 10.8.1, BD Biosciences (BD), Franklin Lakes, NJ, USA).

4.5. ADCC

Five-week-old female BALB/c nude mice were purchased from Jackson Laboratory Japan (Kanagawa, Japan). The splenocytes were prepared as described previously [60] and resuspended in DMEM supplemented with 10% FBS (designated as effector cells). Target cells (CHO/HER2, BT-474, and SK-BR-3) were labeled with 10 µg/mL of Calcein AM (Thermo). The target cells were plated in 96-well plates at a density of 1×10^4 cells/well and combined with effector cells (effector-to-target ratio, 50:1) and 100 µg/mL of either control human IgG₁, trastuzumab, or humH₂Mab-250. After incubating for 4.5 h, the calcein released into the supernatant was measured as described previously [42]. Human NK cells were obtained from Takara Bio, Inc. (Shiga, Japan) and were used immediately after thawing. The target cells were plated in 96-well plates (8×10^3 cells/well) and mixed with the human NK cells (effector to target ratio, 50:1) and 100 µg/mL of either control human IgG₁, trastuzumab, or humH₂Mab-250. The calcein release was measured after incubation for 4.5 h, as described previously [42].

4.6. CDC

The target cells labeled with Calcein AM (CHO/HER2, BT-474, and SK-BR-3) were seeded and combined with rabbit complement (final concentration 15%, Low-Tox-M Rabbit Complement; Cedarlane Laboratories, Hornby, ON, Canada) along with 100 µg/mL of either control human IgG₁, trastuzumab, or humH₂Mab-250. After a 4.5-h incubation at 37 °C, the amount of calcein released into the medium was measured as described previously [42].

4.7. Antitumor Activity of humH₂Mab-250 in Xenografts of CHO/HER2, BT-474, and SK-BR-3

Each cell was first suspended in 0.3 mL of DMEM at a concentration of 1.33×10^8 cells/mL and then combined with 0.5 mL of BD Matrigel Matrix Growth Factor Reduced (BD). BALB/c nude mice were subcutaneously injected with 100 μ L of this mixture (containing 5×10^6 cells) into the left flank. On day 7 post-injection, the mice were treated with 100 μ g of either control human IgG₁ (n = 8), trastuzumab (n = 8), or humH₂Mab-250 (n = 8) via intraperitoneal injection. The treatment was repeated on days 14 and 21. Tumor size was measured and the tumor volume was calculated using the formula $\text{volume} = W^2 \times L/2$, where W represents the width (short diameter), and L represents the length (long diameter). All mice were sacrificed by cervical dislocation on day 28 (CHO/HER2) or day 27 (CHO-K1, BT-474 and SK-BR-3) following tumor cell inoculation.

4.8. Statistical Analyses

Data are presented as the mean \pm standard error of the mean (SEM). Statistical analyses for ADCC, CDC, and tumor weight were performed using one-way ANOVA followed by Tukey's multiple comparisons test. Two-way ANOVA with Tukey's multiple comparisons test was applied to measure tumor volume and mouse weight. A *p*-value of less than 0.05 was considered statistically significant.

5. Conclusions

A humanized cancer-specific anti-HER2 mAb, humH₂Mab-250, exhibited *in vitro* ADCC and CDC activities and showed compatible *in vivo* antitumor effects against breast cancer xenografts with trastuzumab. These findings highlight the clinical development of humH₂Mab-250, including monotherapy, ADC, and CAR-T, with lower side effects for patients with HER2-positive tumors.

Supplementary Materials: The following supporting information can be downloaded at <https://www.mdpi.com/article/10.3390/ijms26031079/s1>.

Author Contributions: Conceptualization, Y.K.; methodology, T.O.; formal analysis, T.T.; investigation, H.S., T.O., T.N., M.Y. and T.T.; data curation, H.S. and Y.K.; writing—original draft preparation, M.K.K. and H.S.; writing—review and editing, Y.K.; project administration, Y.K.; funding acquisition, M.K.K., H.S., T.T. and Y.K. All authors have read and agreed to the published version of the manuscript.

Funding: This research was supported in part by the Japan Agency for Medical Research and Development (AMED) under Grant Numbers 24am0521010 (to Y.K.), JP24ama121008 (to Y.K.), JP24ama221339 (to Y.K.), JP23am0401013 (to Y.K.), JP23bm1123027 (to Y.K.), and JP23ck0106730 (to Y.K.), and by the Japan Society for the Promotion of Science (JSPS) Grants-in-Aid for Scientific Research (KAKENHI) grant nos. 22K06995 (to H.S.), 21K20789 (to T.T.), 21K07168 (to M.K.K.), and 22K07224 (to Y.K.).

Institutional Review Board Statement: The Institutional Committee for Experiments of the Institute of Microbial Chemistry approved animal experiments (approval no. 2024-059, approval date: 7 August 2024).

Informed Consent Statement: Not applicable.

Data Availability Statement: The data presented in this study are available in the article and Supplementary Materials.

Conflicts of Interest: The authors have no conflicts of interest to declare.

References

1. Mullard, A. FDA approves 100th monoclonal antibody product. *Nat. Rev. Drug Discov.* **2021**, *20*, 491–495. [[CrossRef](#)] [[PubMed](#)]
2. Pedrioli, A.; Oxenius, A. Single B cell technologies for monoclonal antibody discovery. *Trends Immunol.* **2021**, *42*, 1143–1158. [[CrossRef](#)]
3. Raja, A.; Kasana, A.; Verma, V. Next-Generation Therapeutic Antibodies for Cancer Treatment: Advancements, Applications, and Challenges. *Mol. Biotechnol.* **2024**. [[CrossRef](#)] [[PubMed](#)]
4. Paul, S.; Konig, M.F.; Pardoll, D.M.; Bettegowda, C.; Papadopoulos, N.; Wright, K.M.; Gabelli, S.B.; Ho, M.; van Elsas, A.; Zhou, S. Cancer therapy with antibodies. *Nat. Rev. Cancer* **2024**, *24*, 399–426. [[CrossRef](#)] [[PubMed](#)]
5. Oh, D.Y.; Bang, Y.J. HER2-targeted therapies—A role beyond breast cancer. *Nat. Rev. Clin. Oncol.* **2020**, *17*, 33–48. [[CrossRef](#)] [[PubMed](#)]
6. Cardoso, F.; Paluch-Shimon, S.; Senkus, E.; Curigliano, G.; Aapro, M.S.; André, F.; Barrios, C.H.; Bergh, J.; Bhattacharyya, G.S.; Biganzoli, L.; et al. 5th ESO-ESMO international consensus guidelines for advanced breast cancer (ABC 5). *Ann. Oncol.* **2020**, *31*, 1623–1649. [[CrossRef](#)]
7. Carter, P.; Presta, L.; Gorman, C.M.; Ridgway, J.B.; Henner, D.; Wong, W.L.; Rowland, A.M.; Kotts, C.; Carver, M.E.; Shepard, H.M. Humanization of an anti-p185HER2 antibody for human cancer therapy. *Proc. Natl. Acad. Sci. USA* **1992**, *89*, 4285–4289. [[CrossRef](#)]
8. Pegram, M.; Hsu, S.; Lewis, G.; Pietras, R.; Beryt, M.; Sliwkowski, M.; Coombs, D.; Baly, D.; Kabbinar, F.; Slamon, D. Inhibitory effects of combinations of HER-2/neu antibody and chemotherapeutic agents used for treatment of human breast cancers. *Oncogene* **1999**, *18*, 2241–2251. [[CrossRef](#)]
9. Pietras, R.J.; Pegram, M.D.; Finn, R.S.; Maneval, D.A.; Slamon, D.J. Remission of human breast cancer xenografts on therapy with humanized monoclonal antibody to HER-2 receptor and DNA-reactive drugs. *Oncogene* **1998**, *17*, 2235–2249. [[CrossRef](#)]
10. Baselga, J.; Norton, L.; Albanell, J.; Kim, Y.M.; Mendelsohn, J. Recombinant humanized anti-HER2 antibody (Herceptin) enhances the antitumor activity of paclitaxel and doxorubicin against HER2/neu overexpressing human breast cancer xenografts. *Cancer Res.* **1998**, *58*, 2825–2831. [[PubMed](#)]
11. Tsao, L.C.; Force, J.; Hartman, Z.C. Mechanisms of Therapeutic Antitumor Monoclonal Antibodies. *Cancer Res.* **2021**, *81*, 4641–4651. [[CrossRef](#)] [[PubMed](#)]
12. Slamon, D.J.; Leyland-Jones, B.; Shak, S.; Fuchs, H.; Paton, V.; Bajamonde, A.; Fleming, T.; Eiermann, W.; Wolter, J.; Pegram, M.; et al. Use of chemotherapy plus a monoclonal antibody against HER2 for metastatic breast cancer that overexpresses HER2. *N. Engl. J. Med.* **2001**, *344*, 783–792. [[CrossRef](#)] [[PubMed](#)]
13. Abrahao-Machado, L.F.; Scapulatempo-Neto, C. HER2 testing in gastric cancer: An update. *World J. Gastroenterol.* **2016**, *22*, 4619–4625. [[CrossRef](#)]
14. Pous, A.; Notario, L.; Hierro, C.; Layos, L.; Bugés, C. HER2-Positive Gastric Cancer: The Role of Immunotherapy and Novel Therapeutic Strategies. *Int. J. Mol. Sci.* **2023**, *24*, 11403. [[CrossRef](#)] [[PubMed](#)]
15. Balestra, A.; Larsimont, D.; Noël, J.C. HER2 Amplification in p53-Mutated Endometrial Carcinomas. *Cancers* **2023**, *15*, 1435. [[CrossRef](#)]
16. Diver, E.J.; Foster, R.; Rueda, B.R.; Growdon, W.B. The Therapeutic Challenge of Targeting HER2 in Endometrial Cancer. *Oncologist* **2015**, *20*, 1058–1068. [[CrossRef](#)] [[PubMed](#)]
17. Garrido-Castro, A.C.; Felip, E. HER2 driven non-small cell lung cancer (NSCLC): Potential therapeutic approaches. *Transl. Lung Cancer Res.* **2013**, *2*, 122–127. [[CrossRef](#)] [[PubMed](#)]
18. Riudavets, M.; Sullivan, I.; Abdayem, P.; Planchard, D. Targeting HER2 in non-small-cell lung cancer (NSCLC): A glimpse of hope? An updated review on therapeutic strategies in NSCLC harbouring HER2 alterations. *ESMO Open* **2021**, *6*, 100260. [[CrossRef](#)]
19. Nasioudis, D.; Gysler, S.; Latif, N.; Cory, L.; Giuntoli, R.L., 2nd; Kim, S.H.; Simpkins, F.; Martin, L.; Ko, E.M. Molecular landscape of ERBB2/HER2 gene amplification among patients with gynecologic malignancies; clinical implications and future directions. *Gynecol. Oncol.* **2024**, *180*, 1–5. [[CrossRef](#)] [[PubMed](#)]
20. Mark, C.; Lee, J.S.; Cui, X.; Yuan, Y. Antibody-Drug Conjugates in Breast Cancer: Current Status and Future Directions. *Int. J. Mol. Sci.* **2023**, *24*, 13726. [[CrossRef](#)]
21. Modi, S.; Saura, C.; Yamashita, T.; Park, Y.H.; Kim, S.B.; Tamura, K.; Andre, F.; Iwata, H.; Ito, Y.; Tsurutani, J.; et al. Trastuzumab Deruxtecan in Previously Treated HER2-Positive Breast Cancer. *N. Engl. J. Med.* **2020**, *382*, 610–621. [[CrossRef](#)] [[PubMed](#)]
22. Shitara, K.; Bang, Y.J.; Iwasa, S.; Sugimoto, N.; Ryu, M.H.; Sakai, D.; Chung, H.C.; Kawakami, H.; Yabusaki, H.; Lee, J.; et al. Trastuzumab Deruxtecan in Previously Treated HER2-Positive Gastric Cancer. *N. Engl. J. Med.* **2020**, *382*, 2419–2430. [[CrossRef](#)]
23. Modi, S.; Jacot, W.; Yamashita, T.; Sohn, J.; Vidal, M.; Tokunaga, E.; Tsurutani, J.; Ueno, N.T.; Prat, A.; Chae, Y.S.; et al. Trastuzumab Deruxtecan in Previously Treated HER2-Low Advanced Breast Cancer. *N. Engl. J. Med.* **2022**, *387*, 9–20. [[CrossRef](#)]
24. Li, B.T.; Smit, E.F.; Goto, Y.; Nakagawa, K.; Udagawa, H.; Mazières, J.; Nagasaka, M.; Bazhenova, L.; Saltos, A.N.; Felip, E.; et al. Trastuzumab Deruxtecan in HER2-Mutant Non-Small-Cell Lung Cancer. *N. Engl. J. Med.* **2022**, *386*, 241–251. [[CrossRef](#)]

25. Mercogliano, M.F.; Bruni, S.; Mauro, F.L.; Schillaci, R. Emerging Targeted Therapies for HER2-Positive Breast Cancer. *Cancers* **2023**, *15*, 1987. [[CrossRef](#)]
26. Lee, K.F.; Simon, H.; Chen, H.; Bates, B.; Hung, M.C.; Hauser, C. Requirement for neuregulin receptor erbB2 in neural and cardiac development. *Nature* **1995**, *378*, 394–398. [[CrossRef](#)]
27. Crone, S.A.; Zhao, Y.Y.; Fan, L.; Gu, Y.; Minamisawa, S.; Liu, Y.; Peterson, K.L.; Chen, J.; Kahn, R.; Condorelli, G.; et al. ErbB2 is essential in the prevention of dilated cardiomyopathy. *Nat. Med.* **2002**, *8*, 459–465. [[CrossRef](#)]
28. Dumontet, C.; Reichert, J.M.; Senter, P.D.; Lambert, J.M.; Beck, A. Antibody-drug conjugates come of age in oncology. *Nat. Rev. Drug Discov.* **2023**, *22*, 641–661. [[CrossRef](#)] [[PubMed](#)]
29. Reis, E.S.; Mastellos, D.C.; Ricklin, D.; Mantovani, A.; Lambris, J.D. Complement in cancer: Untangling an intricate relationship. *Nat. Rev. Immunol.* **2018**, *18*, 5–18. [[CrossRef](#)]
30. Beurskens, F.J.; Lindorfer, M.A.; Farooqui, M.; Beum, P.V.; Engelberts, P.; Mackus, W.J.; Parren, P.W.; Wiestner, A.; Taylor, R.P. Exhaustion of cytotoxic effector systems may limit monoclonal antibody-based immunotherapy in cancer patients. *J. Immunol.* **2012**, *188*, 3532–3541. [[CrossRef](#)] [[PubMed](#)]
31. Lin, T.S. Ofatumumab: A novel monoclonal anti-CD20 antibody. *Pharmgenom. Pers. Med.* **2010**, *3*, 51–59. [[CrossRef](#)]
32. Manches, O.; Lui, G.; Chaperot, L.; Gressin, R.; Molens, J.P.; Jacob, M.C.; Sotto, J.J.; Leroux, D.; Bensa, J.C.; Plumas, J. In vitro mechanisms of action of rituximab on primary non-Hodgkin lymphomas. *Blood* **2003**, *101*, 949–954. [[CrossRef](#)] [[PubMed](#)]
33. Di Gaetano, N.; Cittera, E.; Nota, R.; Vecchi, A.; Grieco, V.; Scanziani, E.; Botto, M.; Introna, M.; Golay, J. Complement activation determines the therapeutic activity of rituximab in vivo. *J. Immunol.* **2003**, *171*, 1581–1587. [[CrossRef](#)]
34. Wang, Y.; Yang, Y.J.; Wang, Z.; Liao, J.; Liu, M.; Zhong, X.R.; Zheng, H.; Wang, Y.P. CD55 and CD59 expression protects HER2-overexpressing breast cancer cells from trastuzumab-induced complement-dependent cytotoxicity. *Oncol. Lett.* **2017**, *14*, 2961–2969. [[CrossRef](#)]
35. Mamidi, S.; Cinci, M.; Hasmann, M.; Fehring, V.; Kirschfink, M. Lipoplex mediated silencing of membrane regulators (CD46, CD55 and CD59) enhances complement-dependent anti-tumor activity of trastuzumab and pertuzumab. *Mol. Oncol.* **2013**, *7*, 580–594. [[CrossRef](#)]
36. de Jong, R.N.; Beurskens, F.J.; Verploegen, S.; Strumane, K.; van Kampen, M.D.; Voorhorst, M.; Horstman, W.; Engelberts, P.J.; Oostindie, S.C.; Wang, G.; et al. A Novel Platform for the Potentiation of Therapeutic Antibodies Based on Antigen-Dependent Formation of IgG Hexamers at the Cell Surface. *PLoS Biol.* **2016**, *14*, e1002344. [[CrossRef](#)]
37. Diebold, C.A.; Beurskens, F.J.; de Jong, R.N.; Koning, R.I.; Strumane, K.; Lindorfer, M.A.; Voorhorst, M.; Ugurlar, D.; Rosati, S.; Heck, A.J.; et al. Complement is activated by IgG hexamers assembled at the cell surface. *Science* **2014**, *343*, 1260–1263. [[CrossRef](#)] [[PubMed](#)]
38. Moore, G.L.; Chen, H.; Karki, S.; Lazar, G.A. Engineered Fc variant antibodies with enhanced ability to recruit complement and mediate effector functions. *MAbs* **2010**, *2*, 181–189. [[CrossRef](#)] [[PubMed](#)]
39. Oostindie, S.C.; van der Horst, H.J.; Kil, L.P.; Strumane, K.; Overdijk, M.B.; van den Brink, E.N.; van den Brakel, J.H.N.; Rademaker, H.J.; van Kessel, B.; van den Noort, J.; et al. DuoHexaBody-CD37^(®), a novel biparatopic CD37 antibody with enhanced Fc-mediated hexamerization as a potential therapy for B-cell malignancies. *Blood Cancer J.* **2020**, *10*, 30. [[CrossRef](#)]
40. Arimori, T.; Mihara, E.; Suzuki, H.; Ohishi, T.; Tanaka, T.; Kaneko, M.K.; Takagi, J.; Kato, Y. Locally misfolded HER2 expressed on cancer cells is a promising target for development of cancer-specific antibodies. *Structure* **2024**, *32*, 536–549.e535. [[CrossRef](#)]
41. Kaneko, M.K.; Suzuki, H.; Kato, Y. Establishment of a Novel Cancer-Specific Anti-HER2 Monoclonal Antibody H(2)Mab-250/H(2)CasMab-2 for Breast Cancers. *Monoclon. Antib. Immunodiagn. Immunother.* **2024**, *43*, 35–43. [[CrossRef](#)] [[PubMed](#)]
42. Suzuki, H.; Ohishi, T.; Tanaka, T.; Kaneko, M.K.; Kato, Y. Anti-HER2 Cancer-Specific mAb, H(2)Mab-250-hG(1), Possesses Higher Complement-Dependent Cytotoxicity than Trastuzumab. *Int. J. Mol. Sci.* **2024**, *25*, 8386. [[CrossRef](#)] [[PubMed](#)]
43. Kaneko, M.K.; Suzuki, H.; Ohishi, T.; Nakamura, T.; Tanaka, T.; Kato, Y. A Cancer-Specific Monoclonal Antibody against HER2 Exerts Antitumor Activities in Human Breast Cancer Xenograft Models. *Int. J. Mol. Sci.* **2024**, *25*, 1941. [[CrossRef](#)] [[PubMed](#)]
44. Inoue, T.; Yamamoto, Y.; Sato, K.; Okemoto-Nakamura, Y.; Shimizu, Y.; Ogawa, M.; Onodera, T.; Takahashi, Y.; Wakita, T.; Kaneko, M.K.; et al. Overcoming antibody-resistant SARS-CoV-2 variants with bispecific antibodies constructed using non-neutralizing antibodies. *iScience* **2024**, *27*, 109363. [[CrossRef](#)] [[PubMed](#)]
45. Yamane-Ohnuki, N.; Kinoshita, S.; Inoue-Urakubo, M.; Kusunoki, M.; Iida, S.; Nakano, R.; Wakitani, M.; Niwa, R.; Sakurada, M.; Uchida, K.; et al. Establishment of FUT8 knockout Chinese hamster ovary cells: An ideal host cell line for producing completely defucosylated antibodies with enhanced antibody-dependent cellular cytotoxicity. *Biotechnol. Bioeng.* **2004**, *87*, 614–622. [[CrossRef](#)] [[PubMed](#)]
46. Shinkawa, T.; Nakamura, K.; Yamane, N.; Shoji-Hosaka, E.; Kanda, Y.; Sakurada, M.; Uchida, K.; Anazawa, H.; Satoh, M.; Yamasaki, M.; et al. The absence of fucose but not the presence of galactose or bisecting N-acetylglucosamine of human IgG1 complex-type oligosaccharides shows the critical role of enhancing antibody-dependent cellular cytotoxicity. *J. Biol. Chem.* **2003**, *278*, 3466–3473. [[CrossRef](#)]

47. Overdijk, M.B.; Verploegen, S.; Ortiz Buijsse, A.; Vink, T.; Leusen, J.H.; Bleeker, W.K.; Parren, P.W. Crosstalk between human IgG isotypes and murine effector cells. *J. Immunol.* **2012**, *189*, 3430–3438. [[CrossRef](#)] [[PubMed](#)]
48. Merle, N.S.; Church, S.E.; Fremeaux-Bacchi, V.; Roumenina, L.T. Complement System Part I—Molecular Mechanisms of Activation and Regulation. *Front. Immunol.* **2015**, *6*, 262. [[CrossRef](#)]
49. Hiemstra, I.H.; Santegoets, K.C.M.; Janmaat, M.L.; De Goeij, B.; Ten Hagen, W.; van Dooremalen, S.; Boross, P.; van den Brakel, J.; Bosgra, S.; Andringa, G.; et al. Preclinical anti-tumour activity of HexaBody-CD38, a next-generation CD38 antibody with superior complement-dependent cytotoxic activity. *EBioMedicine* **2023**, *93*, 104663. [[CrossRef](#)]
50. Diwanji, D.; Trenker, R.; Thaker, T.M.; Wang, F.; Agard, D.A.; Verba, K.A.; Jura, N. Structures of the HER2-HER3-NRG1beta complex reveal a dynamic dimer interface. *Nature* **2021**, *600*, 339–343. [[CrossRef](#)] [[PubMed](#)]
51. Wagner, D.L.; Fritsche, E.; Pulsipher, M.A.; Ahmed, N.; Hamieh, M.; Hegde, M.; Ruella, M.; Savoldo, B.; Shah, N.N.; Turtle, C.J.; et al. Immunogenicity of CAR T cells in cancer therapy. *Nat. Rev. Clin. Oncol.* **2021**, *18*, 379–393. [[CrossRef](#)] [[PubMed](#)]
52. Nie, Y.; Lu, W.; Chen, D.; Tu, H.; Guo, Z.; Zhou, X.; Li, M.; Tu, S.; Li, Y. Mechanisms underlying CD19-positive ALL relapse after anti-CD19 CAR T cell therapy and associated strategies. *Biomark. Res.* **2020**, *8*, 18. [[CrossRef](#)]
53. An, L.; Lin, Y.; Deng, B.; Yin, Z.; Zhao, D.; Ling, Z.; Wu, T.; Zhao, Y.; Chang, A.H.; Tong, C.; et al. Humanized CD19 CAR-T cells in relapsed/refractory B-ALL patients who relapsed after or failed murine CD19 CAR-T therapy. *BMC Cancer* **2022**, *22*, 393. [[CrossRef](#)]
54. Michelozzi, I.M.; Gomez-Castaneda, E.; Pohle, R.V.C.; Cardoso Rodriguez, F.; Sufi, J.; Puigdevall Costa, P.; Subramaniam, M.; Kirtsios, E.; Eddaoudi, A.; Wu, S.W.; et al. Activation priming and cytokine polyfunctionality modulate the enhanced functionality of low-affinity CD19 CAR T cells. *Blood Adv.* **2023**, *7*, 1725–1738. [[CrossRef](#)]
55. Caraballo Galva, L.D.; Jiang, X.; Hussein, M.S.; Zhang, H.; Mao, R.; Brody, P.; Peng, Y.; He, A.R.; Kehinde-Ige, M.; Sadek, R.; et al. Novel low-avidity glypican-3 specific CARTs resist exhaustion and mediate durable antitumor effects against HCC. *Hepatology* **2022**, *76*, 330–344. [[CrossRef](#)] [[PubMed](#)]
56. Hoseini, S.S.; Dobrenkov, K.; Pankov, D.; Xu, X.L.; Cheung, N.K. Bispecific antibody does not induce T-cell death mediated by chimeric antigen receptor against disialoganglioside GD2. *Oncoimmunology* **2017**, *6*, e1320625. [[CrossRef](#)]
57. Zhang, Y.; Patel, R.P.; Kim, K.H.; Cho, H.; Jo, J.C.; Jeong, S.H.; Oh, S.Y.; Choi, Y.S.; Kim, S.H.; Lee, J.H.; et al. Safety and efficacy of a novel anti-CD19 chimeric antigen receptor T cell product targeting a membrane-proximal domain of CD19 with fast on- and off-rates against non-Hodgkin lymphoma: A first-in-human study. *Mol. Cancer* **2023**, *22*, 200. [[CrossRef](#)] [[PubMed](#)]
58. Hosking, M.; Shirinbak, S.; Omilusik, K.; Chandra, S.; Gentile, A.; Kennedy, S.; Loter, L.; Ibitokou, S.; Ecker, C.; Brookhouser, N.; et al. 268 Development of FT825/ONO-8250: An off-the-shelf CAR-T cell with preferential HER2 targeting and engineered to enable multi-antigen targeting, improve trafficking, and overcome immunosuppression. *J. Immunotherapy Cancer* **2023**, *11*, A307. [[CrossRef](#)]
59. Pawluczakowycz, A.W.; Beurskens, F.J.; Beum, P.V.; Lindorfer, M.A.; van de Winkel, J.G.; Parren, P.W.; Taylor, R.P. Binding of submaximal C1q promotes complement-dependent cytotoxicity (CDC) of B cells opsonized with anti-CD20 mAbs ofatumumab (OFA) or rituximab (RTX): Considerably higher levels of CDC are induced by OFA than by RTX. *J. Immunol.* **2009**, *183*, 749–758. [[CrossRef](#)] [[PubMed](#)]
60. Suzuki, H.; Ohishi, T.; Tanaka, T.; Kaneko, M.K.; Kato, Y. A Cancer-Specific Monoclonal Antibody against Podocalyxin Exerted Antitumor Activities in Pancreatic Cancer Xenografts. *Int. J. Mol. Sci.* **2023**, *25*, 161. [[CrossRef](#)] [[PubMed](#)]

Disclaimer/Publisher’s Note: The statements, opinions and data contained in all publications are solely those of the individual author(s) and contributor(s) and not of MDPI and/or the editor(s). MDPI and/or the editor(s) disclaim responsibility for any injury to people or property resulting from any ideas, methods, instructions or products referred to in the content.